Bull. Chem. Soc. Jpn., **76**, 569–574 (2003)

The Layer Structure in Smectic A Phases and the Phase Transition Behavior for Cyano- and Nitrofuran Compounds

Takeyasu Tasaka, Hiroaki Okamoto,* Yuki Morita, Koichi Abe, Kazuo Kasatani, and Shunsuke Takenaka

Department of Advanced Materials Science and Engineering, Faculty of Engineering, Yamaguchi University, Ube, Yamaguchi 755-8611

(Received August 27, 2002)

The layer structure and phasetransition behavior of smectic A phases for 4-(4-alkoxyphenoxycarbonyl)phenyl 5-X-furan-2-carboxylates (X = CN, NO_2) were examined by a small-angle X-ray diffraction method. The higher homologs of both compounds exhibit two kinds of smectic A (Sm A) phases and experience the Sm A-Sm A transition. One Sm A phase exhibited at a higher temperature region having a layer spacing of 1.5–1.9 times the calculated molecular length; and the layer spacing gradually increases with decreasing temperature. The other Sm A phase exhibited at a lower temperature region having a layer spacing of twice the calculated molecular length; also, the layer spacing is almost independent of the temperature. The Sm A–Sm A transition behavior is discussed.

It has been known that many liquid crystal (LC) materials having a polar group, such as a cyano or a nitro group, at the terminal position of the LC core frequently exhibit a complex polymesomorphism involving reentrant nematic and some smectic A and C phases. In such systems, polar interactions involving dipoles arising from the polar group have been supposed to be responsible for complex polymesomorphism.[1] In the most cases, the polar group attaches at the terminal position of the LC core and arranges to be parallel to the long molecular axis; therefore, the dipole-dipole interaction would be helpful for an antiparallel arrangement of molecules.

On the other hand, many LC materials having a polar group at the lateral position of the LC core have been developed. Although some LC materials incorporating a lateral nitro group have been known to exhibit an interesting phase behavior,[2–5] the formation of such a dimer due to polar interactions has not been confirmed, and the effect on the LC properties is not clear.

These facts suggest that the lateral polar substituent has a different function for the LC properties. We have already reported that 4-(4-alkoxyphenoxycarbonyl)phenyl 5-cyanofuran-2-carboxylates (**1**) and 5-nitrofuran-2-carboxylates (**2**) have the mesomorphic sequence of a crystal (C)–Sm A–Sm A–nematic (N)–isotropic (I) type in higher homologs[6–8] (Fig. 1).

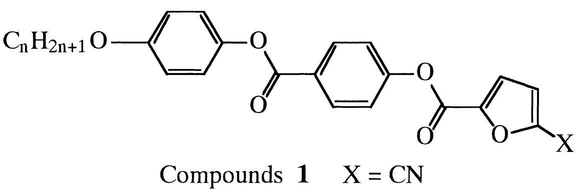

Compounds **1** X = CN
2 X = NO_2

Fig. 1. Molecular structures (n = 7–10).

Although the cyano and nitro groups in these compounds are substituted at the terminal position of the LC core, the average axis of the substituent has an angle of ca. 40° to the long axis of the LC core, due to an intrinsic bent nature of the furan ring. Therefore, LC materials, **1** and **2**, are expected to give useful information concerning polar interactions around the terminal position of the LC core. The layer structure of two Sm A phases and the phasetransition behavior were examined by a small-angle X-ray diffraction method. The phase-transition behavior and layer structure will be discussed in terms of the molecular structure and the polar interaction.

Experimental

Materials and Method. Compounds **1** and **2** were prepared by a conventional method described in our earlier paper.[6–8] X-ray diffraction experiments for the Sm A phases were performed using a Rigaku-denki RINT 2200 diffractometer, where Cu Kα (λ = 1.541 Å) was used as an X-ray source. The reflection angle was calibrated by a comparison of both right and left angles. The temperature was controlled using a Rigaku PTC-20A controller. The samples filled into a quartz capillary (1.5 mmϕ) were oriented by a constant magnetic field (480 G). The samples were heated to the isotropic temperature, and measurements were carried out during the cooling process. The molecular length was calculated by a semi-empirical molecular orbital calculation (MOPAC 97), where minimization of the heat of formation was achieved by an AM1 method.

Results and Discussion

Thermal Properties. The higher homologs of both **1** and **2** show two kinds of Sm A phases and experience the Sm A–Sm A transition, where the Sm A phases exhibited at higher and lower temperature regions are abbreviated as Sm A(1) and Sm A(2), respectively. Both the Sm A phases fundamentally have a focal conic fan texture, while the textures of the Sm

Table 1. Transition Temperatures and Latent Heats for **1** and **2**

Compounds		Transition temperature/°C									Latetnt heat kJ mol^{-1}		
	n	C		Sm A(2)		Sm A(1)		N		I	ΔH_1	ΔH_2	ΔH_3
1[a)]	6	•	139	(•	126)	—		•	153	•	3.2		0.9
	7	•	137	(•	133)	—		•	147	•	4.0		0.9
	8	•	135	•	140	•	141	•	147	•	3.3[c)]		1.0
	9	•	134	•	142	•	144	•	145	•	1.9	1.5	1.7
	10	•	135	•	144	•	148	—		•	2.8	3.3	
2[b)]	6	•	147	—		—		•	172	•			1.1
	7	•	140	(•	128)	•	141	•	169	•	d)	0	1.4
	8	•	139	(•	133)	•	165	•	173	•	1.7	0.1	2.2
	9	•	138	(•	134)	•	173	—		•	1.3	2.7	

C, Sm A, N, and I indicate crystal, smectic A, nematic, and isotropic phases. Prarentheses indicate a monotropic transition. ΔH_1, ΔH_2, and ΔH_3 indicate the latent heats for Sm A(2)–Sm A(1) or N, Sm A(1)–N or I, and N–I transitions, respectively. a) cited from Refs. 6 and 7. b) cited from Ref. 8. c) The latent heats for ΔH_1 and ΔH_2 could not be separated by DSC thermogram due to the narrow range of the Sm A(1) temperature. d) The latent heat could not be evaluated by DSC thermogram due to the large endotherm for the C–Sm A(2) transition.

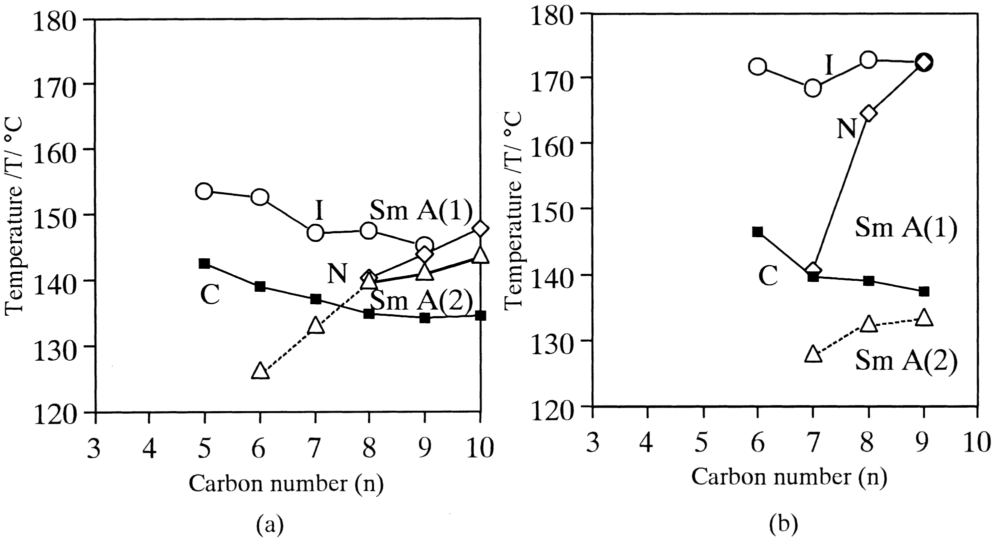

(a)

(b)

Fig. 2. Plots of transition temperature vs. carbon number *n* for: (a); **1** and (b); **2**. C, Sm A, N, and I indicate crystal, smectic A, nematic, and isotropic phases, respectively. Dashed line indicates a monotropic transition.

A(2) upon heating and cooling processes are different from each other due to paramorphism. The transition temperatures and latent heats for **1** and **2** are summarized in Table 1, where most of the values are cited from Refs. 6–8.

For compounds **1**, the Sm A(1) and Sm A(2) phases commence from the hexyloxy and octyloxy homologs, respectively, and the Sm A(2)–Sm A(1) and Sm A(1)–N or I transition points increase parallel to each other upon ascending the homolog. The latent heat for the Sm A(2)–N or Sm A(1) transition is large enough to detect the transition by the DSC thermogram.

For compounds **2**, the Sm A(1) and Sm A(2) phases commence from the heptyloxy homolog, and the Sm A(1)–N or I transition point steeply increases upon ascending the homolog, while the Sm A(2)–Sm A(1) transition point stays almost constant, giving a wide-range Sm A(1) phase. The latent heat for the Sm A(2)–Sm A(1) transition is also large, and tends to increase upon ascending the homolog. These results suggest that the Sm A(2)–Sm A(1) transition has a first-order transition nature.

The transition temperatures are plotted against the carbon number in Fig. 2. A noteworthy fact is that the N or Sm A(1)–I transition points for **2** are higher by ca. 30 °C than those of **1**, resulting in the appearance of a wide-range Sm A(1) phase. Incidentally, the N–I transition points for the cyano compounds, X = COO, OOC, Y = COO, OOC, in Fig. 3 are higher than those for the nitro ones.[9] The difference in the clearing point may be concerned with the geometrical circumstance around the cyano and nitro groups at the terminal position, as

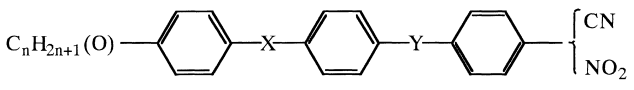

Fig. 3. Molecular structures of benzoate derivative.

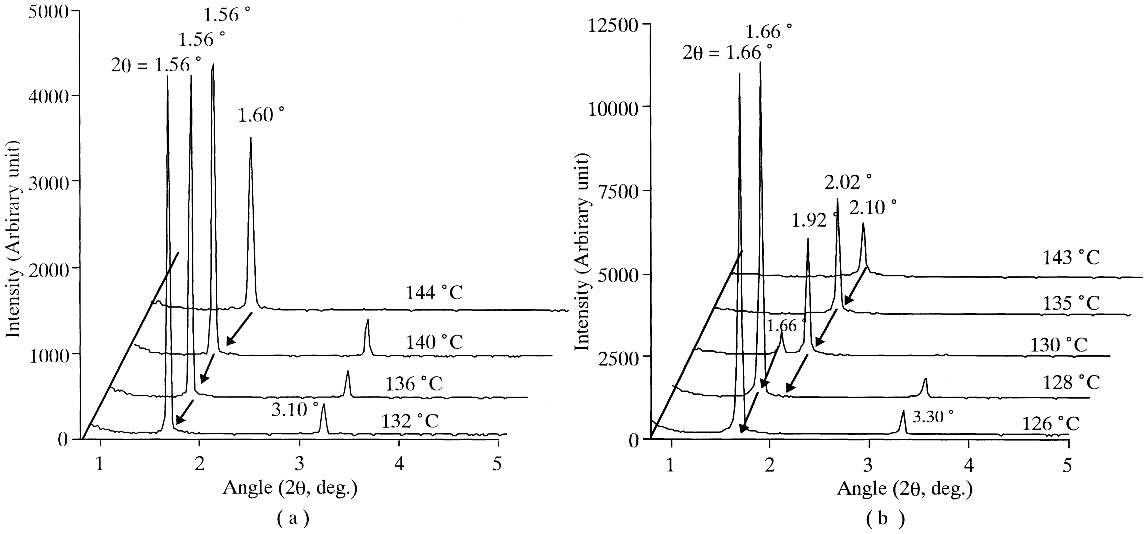

Fig. 4. X-ray profiles for: (a); the nonyloxy homolog of **1**, and (b); heptyloxy one of **2**.

discussed in a later part.

X-ray Diffraction Studies. The phasetransition behavior and layer structure of the Sm A phases were further characterized by a small-angle X-ray diffraction measurement. The X-ray profiles for both Sm A phases consist of two reflection peaks: that is, one is a sharp and high intense reflection which appears in the range between $2\theta = 1.5$ and 3.5°, and the other is a broad one around $2\theta = 20°$. The layer spacing of the Sm A phases were calculated from the former reflection peak, and the appearance of the latter suggests that the molecular arrangement within the smectic layers is disordered, and that these phases are classified into the Sm A modification. Examples are shown in Fig. 4.

For the nonyloxy homolog of **1** in Fig. 4a, the intense reflection peak at $2\theta = 1.60°$ (55.2 Å) appears at the boundary of the N–I and Sm A(1)–N transition points, and the intensity becomes ever-more strong with decreasing temperature. Below 141 °C, a second reflection peak appears at $2\theta = 3.10°$ (28.5 Å). Both reflection angles almost stay constant throughout the temperature range. A similar trend could be observed in the other homologs of **1**.

For the heptyloxy homolog of **2** in Fig. 4b, on the other hand, a weak reflection peak arising from the smectic layer is observed at $2\theta = 2.10°$ even in the N phase, and its intensity becomes large with decreasing temperature in the Sm A(1) phase, and the reflection angle gradually shifts to 1.92°. Interestingly, the intensity of the reflection peak at $2\theta = 1.92°$ suddenly becomes weak in the range between 128 and 130 °C, and simultaneously a new peak at $2\theta = 1.66°$ appears at 130 °C. The intensity of the new reflection peak steeply increases and the peak at $2\theta = 1.92°$ disappears completely at 128 °C, as shown in Fig. 4b. The reflection peaks at $2\theta = 1.66°$ and 2.10° arise from the layer structures of the Sm A(2) and A(1) phases, respectively. These results indicate that two kinds of layer structures competitively co-exist near the Sm A(2)–Sm A(1) transition point between 128 and 130 °C, and the distribution rapidly changes near the boundary of the phase transition point at 128 °C.

Probably, such a replacement of the layer structures does not occur in **1**, since the growth of the layer structure of both the Sm A(2) and Sm A(1) phases would be insufficient in the narrow temperature range of 3 °C (Sm A(2)•142•Sm A(1)•144•N•145•I), and these layer structures might co-exist as the domains in the N phase. The phasetransition behavior might resemble the Sm A_2–Sm A_d–N transition of the heptyl and heptyloxy homologs of 4-R-phenyl 4-(4-cyanobenzoyloxy)benzoates (R = C_7H_{15} or OC_7H_{15}, X, Y = OOC, in Fig. 3).[10,11] Both compounds exhibit the Sm A_d phase being sandwiched between N and Sm A_2 ones, and the temperature range of the Sm A_d phase is narrow. In these compounds, the latent heat for the Sm A_2–Sm A_d transition point has been reported to be large, and the transitions are supposed to have a trace of the first-order nature.

The layer spacings calculated from the peak top of the reflection are plotted against temperature in Fig. 5. For compounds **1** in Fig. 5a, the layer spacing gradually increases with decreasing temperature and stays constant in the Sm A(2) range. The layer spacing appears to vary continuously near the Sm A(1)–Sm A(2) transition point, indicated by the arrow. Interestingly, the layer spacing in the Sm A(1) phase resembles that in the Sm A(2) phase. The layer spacing of the weak reflection peak which appeared near 30 Å is almost independent of the temperature.

On the other hand, the layer spacing for **2** gradually increases within the Sm A(1) phase, and shows a notable change near the Sm A(2)–Sm A(1) transition point. Considering the fact that a discontinuous molecular rearrangement occurs near the Sm A(2)–Sm A(1) transition point, as mentioned above, the actual change of the layer spacing in the Sm A(1) phase may not be very large, while the apparent change in the layer spacing in the Sm A(1) phase is notable, as shown in Fig. 5b. On the other hand, the layer spacing in the Sm A(2) phase remains constant, similar to that of **1**.

In order to consider more exactly the molecular arrangement in the Sm A phases, the molecular structure was estimated by a semi-empirical molecular orbital method (MOPAC97), where minimization of the heat of formation was achieved by an AM1 method. The entire molecular shape and the longitu-

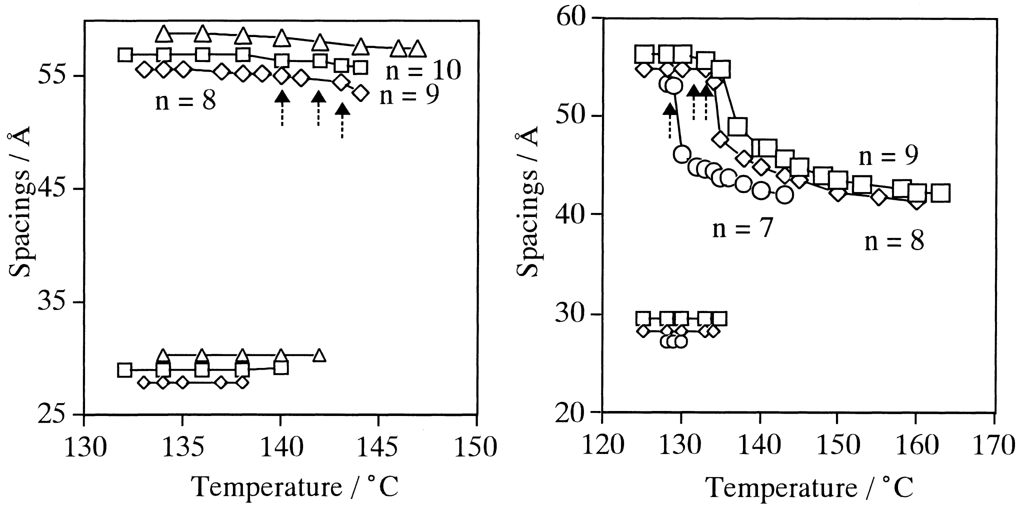

(a) (b)

Fig. 5. Plot of layer spacing vs temperature for: (a); **1** and (b); **2**. *n* indicate the carbon number of the alkoxy chain.

dinal length are mainly determined by the relative orientation of the terminal alkoxy, two ester groups, and furan involving the cyano or the nitro one, where we supposed that the alkoxy group has a zigzag conformation so as to keep the best linearity. Because the energy difference between conformers having a different conformation around the alkoxy and two ester groups is small,[12] it was supposed that the molecule keeps the best linearity, as shown in Fig. 6.

In the model, two extreme conformers, A and B, are possible with respect to the furan–COO bond. The MO calculation suggests that conformer B is more stable by 3.1 and 3.6 kJ/mol than A for the cyano and nitro derivatives, respectively. The electrostatic interactions between the carbonyl group of the ester linkage and the lone-pair electrons of the furan oxygen may be responsible for the energy difference. In any case, the energy difference between both conformers is enough to shift the rotational isomerism to conformer B. As we can assume from the figures, the terminal cyano or the nitro group notably tilts from the average axis of the LC core. Protrusion of the nitro or the cyano group and the increased diameter around the furan moiety are assumed to be responsible for the reduction of the N–I transition point.

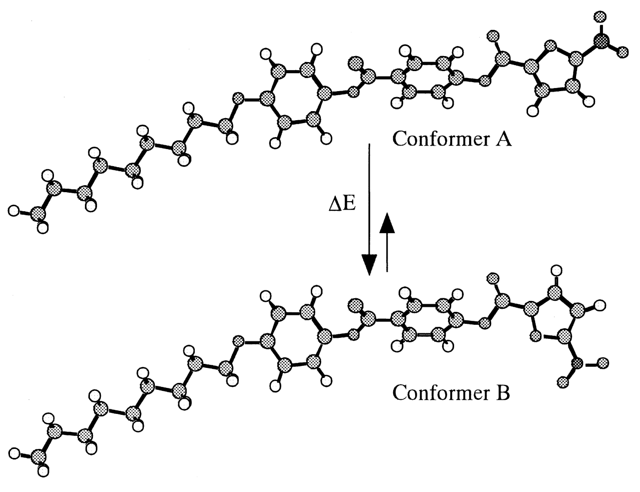

Fig. 6. Two extreme conformers for the nonyloxy homolog of **2**. ΔE indicates the difference in the heat of formation for conformers **A** and **B**, calculated by MOPAC97. ΔE's are 3.1 and 3.6 kJ/mol for **1** and **2**, respectively.

For the nonyloxy homolog of **2**, the longitudinal lengths for conformers A and B are calculated to be 30.2 and 29.0 Å, respectively. Similarly, the longitudinal lengths for conformers A and B are 30.3 and 29.0 Å for the nonyloxy homolog of **1**. In practice, however, the molecular length is an average of many conformers involving extreme conformers A and B. We supposed that conformer B preferentially exists in the Sm A phases, and the longitudinal molecular lengths of **1** and **2** were calculated from conformer B. The calculated molecular length and layer spacing are plotted against the carbon number in Fig. 7. Supposing that molecules form a monolayer arrangement in the Sm A phase, and the average axis of the alkoxy group arranges orthogonal to the smectic layer, the layer spacing is expected to increase by 1.25 Å/CH$_2$, as shown in the figure (■).

For compounds **1**, the plot for the reflection peak near 55 Å gives a slope of 1.7 Å/CH$_2$. Although the slope is smaller than 2.5 Å, twice that of 1.25 Å, and the layer spacings for the homologs are shorter than twice the calculated molecular lengths; the molecular arrangement in the Sm A(2) phase is assumed to be a bilayer one. In addition, the homologs exhibit a weak reflection near 30 Å, and the plot in Fig. 7 gives a slope of 1.4 Å/CH$_2$. This result suggests that a monolayer arrangement also exists in the Sm A(2) phase, while the layer spacings are slightly shorter than the calculated molecular lengths. Considering the fact that the reflection peak near 55 Å is very intense compared with 30 Å, both monolayer and bilayer arrangements competitively exist in the Sm A(2) phase, where the bilayer arrangement is predominant. Because the Sm A(2) phase for **2** shows a similar phase behavior, the bilayer arrangement is predominant in this phase.

Generally, Sm A$_1$ and SmA$_2$ phases are different from a thermodynamic point of view, and the Sm A$_1$–SmA$_2$ phase transition has been supposed to occur directly, or through a rib-

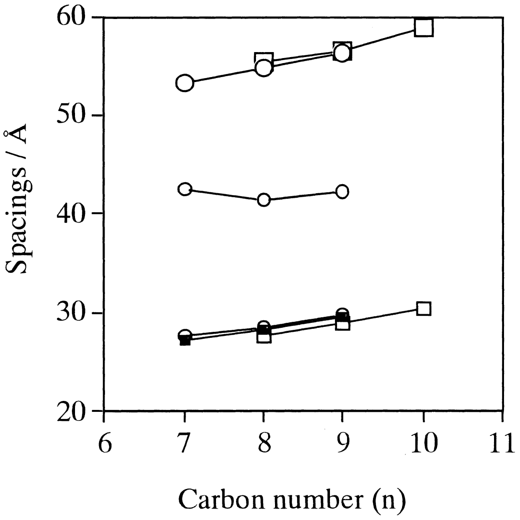

Fig. 7. Plots of layer spacing and calculated molecular length vs. carbon number *n*. The layer spacing in Sm A phases for **1** (□) and **2** (○). The calculated molecular length for conformer **B** of **2** (■).

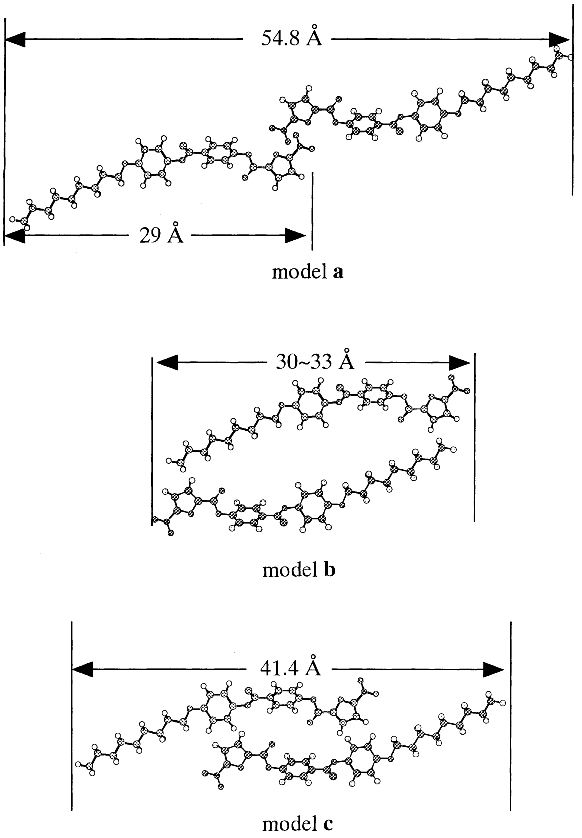

Fig. 8. Possible molecular arrangements in Sm A phases for the nonyloxy homolog of **2**.

bon phase.[13–15] The molecular arrangements in the Sm A_2, A_1, and A_d phases are schematically shown in Fig. 8. In models **a** and **b**, corresponding to the Sm A_2 and A_1 phases, respectively, the nitro or the nitrofuran moieties arrange side by side. For models **a** and **b**, the nitro groups cohere around the surface of the smectic layer, and are closely placed, probably, 1–3 Å, so that inter-layer interactions around the nitro groups would promote and stabilize the layer structure. In our previous paper, we described that dissymmetric LC materials having a terminal halogen, trifluoromethyl, and trifluoromethoxy groups tend to exhibit the Sm A phase, where the layer spacing is 2–5 Å longer than the calculated molecular length; a similar molecular arrangement to model **b** has been postulated.[16] According to the conventional classification, the Sm A_1 phase having model **b** is classified into a "polar" Sm A_1 one.

The Sm A phase of the model **b** type is also exhibited by some members of cyanophenyl and nitrophenyl compounds: X, Y = COO, X, Y = OOC, X = COO and Y = OOC in Fig. 3.[17] On the other hand, the layer spacing in the Sm A(1) phase for **2** is also longer than the calculated molecular length. The ratios of the layer spacing to the calculated molecular length for the heptyloxy, octyloxy, and nonyloxy homologs are 1.5, 1.4, and 1.4, respectively, close to those for the Sm A_d phase of 4-cyanobiphenyl and 4-cyanophenyl compounds.[18–21]

For the phenomena, the formation of an anti-parallel dimer, model **c** in Fig. 8, has been supposed. Compounds **2** may also form a similar arrangement in the Sm A(1) phase. However, model **c** is fundamentally different from models **a** and **b**, since the polar interactions around the nitro groups within the "dimer" should be very weak compared with those in models **a** and **b**, since both nitro groups within the dimer are far apart; that is, the distance between the nitro groups is assumed to be ca. 10 Å from model **c**. Therefore, the basic forces for the formation of the molecular arrangement have been in a fog. Considering the fact that the formation of the Sm A_d phase is strongly dependent not only on the terminal polar group, but also on the alkoxy chain length, we think that a subtle difference in the entire molecular shape must be taken very carefully into consideration, in connection with the molecular packing.

From a structural point of view, the transition from the Sm A_d to Sm A_2 or Sm A_1 phases should be of the first-order type and accompany a large change in the molecular rearrangement.[10,11]

On the other hand, the layer spacings in the Sm A(1) phase for octyloxy, nonyloxy, and decyloxy homologs of **1** are 54.8, 55.6, and 57.3 Å near the Sm A(1)–N or the N–I transition point, respectively, and are almost twice of the calculated molecular length. These results indicate, therefore, that the layer structure in the Sm A(1) phase resembles model **a** rather than **c**. In practice, however, the longer layer spacing in the Sm A(1) phase in appearance is assumed to be a consequence of the competitive formation of both molecular arrangements in models **a** and **c**.

We have already reported that a reentrant N phase appears in some binary mixtures consisting of the homologs of **1** and nonpolar LC compounds.[7,8] Consequently, the Sm A(1) phase is classified into the Sm A_d modification, from a thermodynamic point of view.

Conclusion

The Sm A(2) phase for **1** has a bilayer arrangement of molecules, where the monolayer one also co-exist as domains, and is classified into the conventional "Sm A_2" one. The Sm A(1) phase should be classified into the conventional "Sm A_d" one, while the layer spacing is ca. twice the molecular length. Probably, the Sm A_2, Sm A_1, and Sm A_d phases competitively exist near the Sm A(2)–Sm A(1)–N transition points. The Sm A(2) phase for **2** also has a bilayer arrangement of molecules, where domains having the monolayer arrangement also coexist, and are classified into the Sm A_2 one. The Sm A(1) phase is classified into the "Sm A_d" phase, where the layer spacing is ca. 1.5 times the molecular length. For these compounds, the Sm A_1 phase is not exhibited as a thermodynamically stable phase.

References

1 G. W. Gray and J. W. Goodby, "Smectic Liquid Crystals," Heyden and Son Inc., Philadelphia (1984), p.134.

2 G. W. Gray, B. Jones, and F. Marson, *J. Chem. Soc.*, **1957**, 393.

3 S. Kutsumizu, T. Ishikawa, S. Nojima, and S. Yano, *Chem. Commun.*, **1999**, 1181.

4 T. Tasaka, H. Okamoto, Y. Morita, K. Kasatani, and S. Takenaka, *Chem. Lett.*, **2002**, 222.

5 H. Sugiura, Y. Sakurai, Y. Masuda, H. Takeda, S. Kusabayashi, and S. Takenaka, *Liquid Crystals*, **3**, 441 (1991).

6 S. Miyake, S. Kusabayashi, and S. Takenaka, *Bull. Chem. Soc. Jpn.*, **57**, 2404 (1984).

7 S. Takenaka, S. Miyake, and S. Kusabayashi, *Mol. Cryst. Liq. Cryst.*, **126**, 211 (1985).

8 S. Takenaka, S. Miyake, and S. Kusabayashi, *Mol. Cryst. Liq. Cryst.*, **131**, 257 (1985).

9 S. Takenaka, Y. Sakurai, H. Takeda, T. Ikemoto, H. Miyake, S. Kusabayashi, and T. Takagi, *Mol. Cryst. Liq. Cryst.*, **178**, 103 (1990).

10 A. M. Levelut, B. Zaghloul, and F. Haudouin, *J. Physique Lett.*, **43**, L-83 (1982).

11 F. Haudouin, M. F. Achard, N. H. Tinh, and G. Sigaud, *J. Physique Lett.*, **46**, L-123 (1985).

12 T. Tasaka, H. Okamoto, V. F. Petrov, and S. Takenaka, *Mol. Cryst. Liq. Cryst.*, **357**, 67 (2001).

13 J. Wang and T. C. Lubensky, *Phys. Rev., A*, **29**, 2210 (1984).

14 H. Fadel, D. Guillon, A. Skoulios, F. Barbarin, and M. Dugay, *J. Phys. (Paris)*, **50**, 375 (1989).

15 M. J. Young, L. Wu, G. Nounesis, C. W. Garland, and R. J. Birgeneau, *Phys. Rev. E*, **50**, 368 (1994).

16 M. Duan, T. Tasaka, H. Okamoto, and S. Takenaka, *Liquid Crystals*, **27**, 1195 (2000).

17 T. Tasaka, Y. Morita, H. Okamoto, K. Kasatani, and S. Takenaka, unpublished results in our laboratory.

18 A. J. Leadbetter, J. C. Frost, J. P. Gaughan, G. W. Gray, and A. Mosley, *J. Physique*, **40**, 375 (1979).

19 J. W. Goodby, T. M. Leslie, P. E. Cladis, and P. L. Finn, "Liquid Crystals and Ordered Fluids," ed by J. F. Johnson and R. S. Porter, Plenum Press, New York (1978), Vol. 3, p. 89.

20 P. E. Cladis, P. L. Finn, and J. W. Goodby, "Liquid Crystals and Ordered Fluids," ed by J. F. Johnson and R. S. Porter, Plenum Press, New York (1978), Vol. 3, p. 203.

21 P. E. Cladis, *Liquid Crystals*, **24**, 15 (1998).